4

New IM Torque Control Scheme with Improved Efficiency and Implicit Rotor Flux Tracking

Bojan Grčar, Peter Cafuta and Gorazd Štumberger
University of Maribor, Faculty of Electrical Engineering and Computer Science
Slovenia

1. Introduction

The induction machine serves as a workhorse in the majority of industrial and commercial applications requiring speed or torque controlled drives. Control design that satisfies a high number of different performance objectives is becoming an increasingly important and challenging issue. Although the research community has proposed several control structures for this purpose, only two major schemes have been accepted by the industry: the well established field-oriented control (FOC) and the more recent direct torque control (DTC).

The popularity and wide applicability of FOC arises from its relatively simple, and decoupled (rotor flux linkage versus torque) structure (Blaschke, 1971). A deeper understanding of FOC performance has been achieved by control theorists, including feedback linearization (Marino, 1999), (Bodson & Chiasson, 1998), (Chiasson, 1998), passivity (Ortega, 1998), and flatness (Martin & Rouchon, 1996). Formal stability proofs, together with guidelines for controller parameter settings, are now available.

The main characteristic of standard FOC, namely invariance of the magnitude of the rotor flux linkage vector, enables a globally stable solution for the non-holonomic (double) integrator problem, which in essential describes the IM rotor dynamics (Brockett, 1996), (Grcar, 2011). Since the FOC concept requires implicit system inversion (mapping of the oriented reference current vector into voltage vector), an inner current loop is needed. An outer loop for speed and/or torque control is usually designed for the reduced model, assuming that high gain current controllers achieve perfect tracking of the current command. Recent results improve the FOC capability and efficiency by explicit rotor field tracking (Peresada, 2003), (Chakraborty & Hori, 2003). It should be pointed out that in all various modifications of FOC some kind of estimator (open-loop) or observer (closed-loop) is required at least for necessary coordinate transformations. Proving rigorously overall global stability based on the estimated variables while considering the rotor flux tracking, current limits and parameter variations is a difficult task and is still an ongoing challenge.

On the other hand, DTC (Takagashi & Noguchi, 1986), (Depenbrock, 1986), introduces a different control philosophy based on stator flux linkage rotation. This concept is voltage-based and operates without explicit current controllers (Ortega, 2000), (Attaianese, 1999). Some authors claim that, by introducing stator quantities into the torque control, substantial reduction in parameter sensitivity is achieved. Control signal (stator voltage vector) is generated in accordance with the finite number of possible voltage-source inverter

(VSI) states, resulting in a complex nonlinear hybrid feedback system. The switching logic can be expressed in the form of algebraic inequalities to enable both stability analysis and determination of feasible operation areas. Some additional performance criteria (minimal losses, best tracking) might be simultaneously satisfied by selecting alternative switching patterns.

In this chapter, we examine a control structure that does not fit in either of the two classes although the proposed control uses a cascaded structure similar to FOC and vector rotation concept along with assumption of known machine torque similar to DTC. Our design is based on an IM model in a reference frame aligned with the stator current vector. Although it is well known that structural machine properties are invariant under different bijective geometric transformations, the choice of the reference frame have indeed some relevant implications in physical interpretation of the control design, especially in practice. The choice of stator current reference frame is justified due to the following facts:

- Dynamic inversion of the rotor dynamics enables the unique determination of maximal torque-per-amp ratio ($T_{el} / \|i_s\|$) equilibrium for all required torques.
- All machine fluxes (stator, air-gap, rotor) have the same torque-producing component, orthogonal to the stator current vector.
- The suggested reference frame enables the determination of a safe operation region delimited by the maximal torque-per-amp ratio thus offering the possibility for implicit rotor flux linkage changes through the manipulation of the stator current vector only.
- The stator current vector is a measured quantity, therefore the corresponding coordinate transformation is parameter invariant.
- In the implementation of the proposed control, only one of the orthogonal flux linkage components is necessary to obtain reliable machine torque estimate. The influence of the parameter uncertainty could be therefore reduced.

We propose that current vector magnitude and its relative rotation speed are changed simultaneously in accordance with the reference torque command so that maximal torque per ampere ratio is achieved for any feasible steady state (assuming perfect knowledge of parameters). Rotor flux linkage vector, not directly used in the proposed torque control scheme, is therefore allowed to change freely in accordance with the actual rotor dynamics. This concept results in a single input-two output system instead of the two input-two output system encountered in other schemes. During transients, the rotor flux linkage vector can be forced to remain close to the maximal torque-per-amp ratio bounds inside the sector of safe operation. This important property is achieved by adjusting amplitude and frequency modulation of the stator current vector. In addition, no singularities restrict the operation at zero state (zero torque, zero flux linkage, zero mechanical speed) or during torque reversal. Assuming that signal conditioning and estimation of the machine torque are solved adequately, almost proportional torque responses are obtained for smooth or even step references except in the obvious case when the machine rotor flux linkage starts near zero state. The problem of static "field weakening" and more demanding flux tracking is therefore solved concurrently for all feasible operating conditions since the machine operates with a minimal rotor flux linkage magnitude needed to generate the required torque. Usually un-modelled saturation effects could be substantially reduced since proposed reference frame is not affected by these effects and the rotor flux linkage is not directly used in the proposed

control scheme. The upper bounds of reachable torque and mechanical speed are given by the current and voltage constraints. Extension towards speed control can be achieved in the standard way, with an additional (PI) control loop. Proposed feedback structure is relatively simple, easy to implement on the standard hardware, and is mostly based on physical considerations.

The organization of the chapter is as follows. First, the IM model in fixed stator $\alpha - \beta$ reference frame is transformed into the reference frame aligned with the stator current vector. In Section 2, a second order nonlinear reduced model, derived from the wide adopted assumption of high gain current controllers, is introduced. Partial dynamical inversion and maximal torque-per-amp ratio equilibrium conditions are presented. We also introduce, for particular initial conditions, a set of guidelines to design our torque controller. In Section 3, the main result introducing several versions of open- or closed-loop torque controller for nominal and perturbed parameter case is given. The inner current loop designed in rotor $\gamma - \delta$ reference frame with almost perfect tracking capability and sufficient robustness is presented in Section 5. Adopting well justified time separation of the stator and rotor dynamics the time-varying linear current controllers based on the internal model principle are introduced. In Section 6, we include different experimental results illustrating the potential and performance characteristics of the proposed IM torque control. In Appendix I detailed stability analysis of the feedback system is presented while in Appendix II the description of the experimental set-up along with motor data and controller parameters are given.

2. IM model in stator current reference frame

Under standard modelling assumptions (Krause, 1986) for linear magnetics and by choosing the stator current vector and the rotor flux linkage vector as state variables, an $\alpha - \beta$ model in a fixed reference frame for the two pole machine is obtained in the form of

$$\begin{bmatrix} \dot{i}_{\alpha\beta} \\ \dot{\psi}_{\alpha\beta} \\ \dot{\omega}_m \end{bmatrix} = \begin{bmatrix} -\tau_\sigma^{-1} i_{\alpha\beta} + \frac{M}{L_\sigma L_r \tau_r}(\mathrm{J}^T \omega_m \tau_r + 1)\psi_{\alpha\beta} + \frac{1}{L_\sigma} u_{\alpha\beta} \\ -\tau_r^{-1}(\mathrm{J}^T \omega_m \tau_r + 1)\psi_{\alpha\beta} + \tau_r^{-1} M i_{\alpha\beta} \\ \frac{M}{JL_r} i_{\alpha\beta}^T \mathrm{J} \psi_{\alpha\beta} - T_L / J \end{bmatrix} \tag{1}$$

Introducing a new set of state variables $z = [\|i_s\|, \theta_i, \psi_I, \psi_\perp, \omega_m]^T$, along with the nonlinear state transformation

$$z = T(x) = \begin{bmatrix} \sqrt{i_\alpha^2 + i_\beta^2} \\ \tan^{-1}(\frac{i_\beta}{i_\alpha}) \\ \cos(\theta_i)\psi_\alpha + \sin(\theta_i)\psi_\beta \\ -\sin(\theta_i)\psi_\alpha + \cos(\theta_i)\psi_\beta \\ \omega_m \end{bmatrix} \tag{2}$$

and with the new input vector

$$\begin{bmatrix} u_I \\ u_\perp \end{bmatrix} = \begin{bmatrix} \cos(\theta_i)u_\alpha + \sin(\theta_i)u_\beta \\ -\sin(\theta_i)u_\alpha + \cos(\theta_i)u_\beta \end{bmatrix} \tag{3}$$

the transformed model ($\dot{z} = \frac{\partial T(x)}{\partial x}\dot{x}$) in the stator current vector reference frame is obtained in the form of

$$\begin{bmatrix} \dot{\|i_s\|} \\ \dot{\theta}_i \\ \dot{\psi}_I \\ \dot{\psi}_\perp \\ \dot{\omega_m} \end{bmatrix} = \begin{bmatrix} -\tau_\sigma^{-1}\|i_s\| + \frac{M}{L_\sigma L_r \tau_r}\psi_I + \omega_m \frac{M}{L_\sigma L_r}\psi_\perp + \frac{1}{L_\sigma}u_I \\ -\omega_m \frac{M}{L_\sigma L_r}\frac{\psi_I}{\|i_s\|} + \frac{M}{L_\sigma L_r \tau_r}\frac{\psi_\perp}{\|i_s\|} + \frac{1}{L_\sigma \|i_s\|}u_\perp \\ -\tau_r^{-1}\psi_I + (\omega_i - \omega_m)\psi_\perp + M\tau_r^{-1}\|i_s\| \\ -\tau_r^{-1}\psi_\perp - (\omega_i - \omega_m)\psi_I \\ -\frac{1}{J}(\frac{M}{L_r}\psi_\perp\|i_s\| - T_L) \end{bmatrix} \tag{4}$$

Assuming that, with some appropriate current controllers, the tracking problem of $\|i_s\|^\star, \omega_i^\star$ can be solved, the reduced second order IM model representing the rotor dynamics is derived as

$$\begin{bmatrix} \dot{\psi}_I \\ \dot{\psi}_\perp \end{bmatrix} = \begin{bmatrix} -\tau_r^{-1}\psi_I + \omega_r\psi_\perp + M\tau_r^{-1}\|i_s\| \\ -\tau_r^{-1}\psi_\perp - \omega_r\psi_I \end{bmatrix} \tag{5}$$

along with the algebraic output equation for the generated electrical torque

$$T_{el} = -\frac{M}{L_r}\psi_\perp\|i_s\| \tag{6}$$

In (5) we introduced relative speed ω_r as the difference between the rotation speed of the stator current vector ω_i and the rotor speed ω_m. In the following, the rotor speed is simply interpreted as a bounded time-varying parameter, and the dynamics of the mechanical part is therefore omitted from further analysis. Considering the reduced model (5), along with the output equation (6) it can be seen that unique inverse mapping $T_{el} \rightarrow \psi_I, \psi_\perp, \|i_s\|, \omega_r$ does not exist. Additional conditions must therefore be introduced to the obtain required equilibrium. By manipulating only the first control input $\|i_s\|$, assuming that $\omega_r = 0$, only the rotor flux linkage component ψ_I will be changed. The second input ω_r must therefore also be changed in order to establish necessary $\psi_\perp$ and thus generate the required machine torque. Since current vector rotation is required for all transient and steady-states (except at $T_{el} = 0$ and $\omega_m = 0$), the corresponding equilibrium conditions must be determined. Steady-state characteristics describing relations between machine torque, stator current vector magnitude and relative speed are given in Fig. 1. Consequently, different control strategies could be

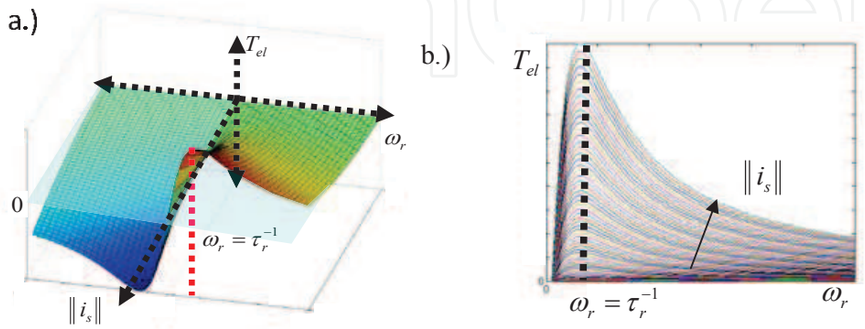

Fig. 1. Steady-state relations between electrical torque T_{el}, stator current vector magnitude $\|i_s\|$ and relative speed ω_r.

employed in the torque generation. Keeping the current vector magnitude constant at some nominal value, high torque dynamics on the cost of reduced torque-per-amp ratio is obtained. On the other hand, if we keep the second input ω_r constant, the efficiency could be improved, but only poor dynamics would be achieved due to the slow dynamics in the rotor flux linkage magnitude. Thus, the real control challenge lies in the question of how to manipulate both control inputs simultaneously to achieve acceptable torque tracking and global stability, as well as the maximal torque-per-amp ratio in steady-state.

3. Partial dynamic inversion

Considering the reduced model (5) and assuming that ω_r is a constant parameter, equation (5) can be written in linear state-space form

$$\dot{\psi}_r = \begin{bmatrix} -\tau_r^{-1} & \omega_r \\ -\omega_r & -\tau_r^{-1} \end{bmatrix} \psi_r + \begin{bmatrix} \tau_r^{-1} M \\ 0 \end{bmatrix} \|i_s\| \tag{7}$$

where $\psi_r = [\psi_I,\, \psi_\perp]^T$. Calculating the corresponding transfer functions

$$\begin{aligned} G_1(s) &= \frac{\psi_I}{\|i_s\|} = \frac{(s\tau_r + 1)M}{s^2\tau_r^2 + 2s\tau_r + 1 + \omega_r^2\tau_r^2} \\ G_2(s) &= \frac{\psi_\perp}{\|i_s\|} = -\frac{\omega_r\tau_r M}{s^2\tau_r^2 + 2s\tau_r + 1 + \omega_r^2\tau_r^2} \end{aligned} \tag{8}$$

we can easily conclude that maximal steady-state gain between $\|i_s\|$ and $\psi_\perp$ is obtained if the following dynamic condition

$$\omega_r = \tau_r^{-1} \tag{9}$$

is satisfied. Note that introduced relative rotation speed ω_r equals the slip speed in the steady-state. Since the quantities $\psi_\perp, \|i_s\|$ are torque producing, this implies that maximal torque per ampere ratio is obtained at any steady-state resulting from the equilibrium condition (9). From steady-state analysis It further follows that

$$\begin{bmatrix} \psi_I \\ \psi_\perp \end{bmatrix} = \begin{bmatrix} \frac{M\|i_s\|}{1+\omega_r^2\tau_r^2} \\ -\frac{\omega_r\tau_r M\|i_s\|}{1+\omega_r^2\tau_r^2} \end{bmatrix} \tag{10}$$

Additional characteristic feature is derived from (10) on condition that (9) is satisfied

$$\psi_I = |\psi_\perp| \tag{11}$$

where ψ_I is restricted to positive values. Furthermore, we can calculate the steady-state torque producing flux linkage vector component and the corresponding current vector magnitude for a given torque command $T_{el}^\star$

$$\begin{aligned} \psi_\perp^\star &= -\text{sign}(T_{el}^\star)\sqrt{\tfrac{|T_{el}^\star|L_r}{2}} \\ \|i_s\|^\star &= \tfrac{2}{M}|\psi_\perp^\star| \end{aligned} \tag{12}$$

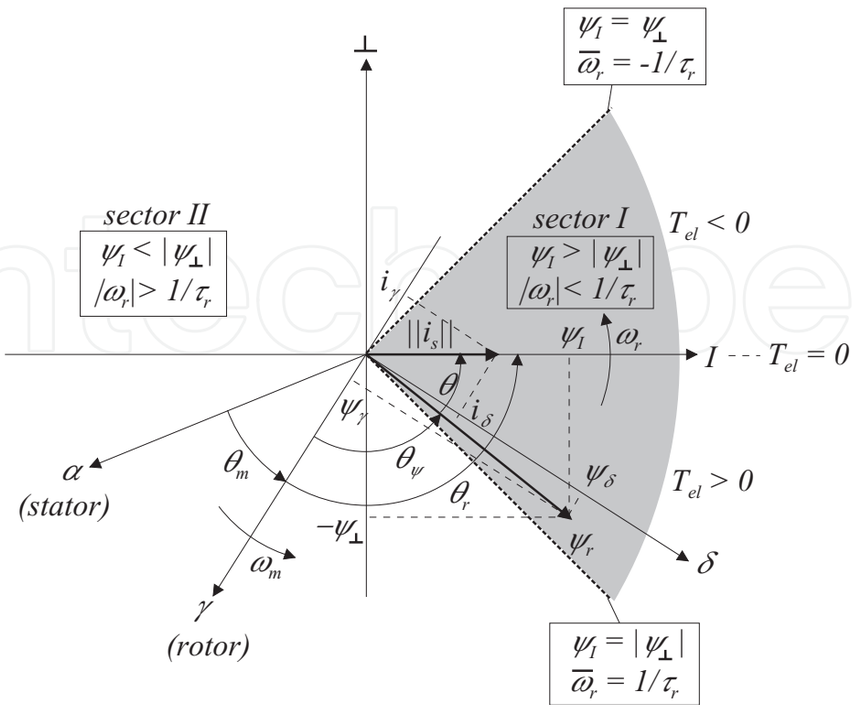

Fig. 2. Desired operating sector I and reference frames.

In Fig. 2 a graphical interpretation of the desired operating sector and the relevant reference frames are given. The trajectories of the rotor flux linkage vector inside the $\pi/2$ wide sector I always ensure torque responses without stall by bounding ω_r. However, only steady-states on the boundary of sector I additionally fulfill the maximal torque-per-amp ratio requirement. Operation in sector II without bounding ω_r is avoided due to oscillatory torque responses and danger of stall.

The control design challenge is to force the flux linkage trajectories to remain predominantly inside sector I during transients and in steady-states to lie as close as possible to the maximal torque-per-amp line. A careful study of (5) allows us to conclude that the rotor flux linkage will remain, for zero initial rotor flux linkage, inside sector I provided the following conditions are satisfied

$$\begin{aligned} &\psi_I \geq |\psi_\perp|; \ \forall T_{el}^\star \\ &\|i_s\| = f(\omega_r) \leq \|i_s\|\text{max} \\ &|\omega_r| \leq \tau_r^{-1} \quad \text{in steady-state} \\ &\dot{\psi}_\perp \leq 0; \ T_{el}^\star > 0 \ \text{ or} \\ &\dot{\psi}_\perp \geq 0; \ T_{el}^\star < 0 \ \text{ or} \\ &\psi_\perp = 0; \ T_{el}^\star = 0 \end{aligned} \tag{13}$$

The analysis of different flux trajectory families resulting from (5), existence of unique equilibrium (9), (11) and (12) along with the introduced conditions (13), motivated us to design the torque controller introduced in the next Section.

4. Torque controller design

The proposed control implies that machine torque is known. Several estimation and measuring techniques are available. Advanced, robust estimation methods use voltage sensors and stator equations (Verghese & Sanders, 1988), (Vas, 1998) and (Briz, 2002) instead of more parameter sensitive rotor estimators. Note that only in the reference frame that is proposed estimation of any (stator, rotor or air-gap) orthogonal flux linkage projection, with the respect to the measured stator current vector magnitude, is sufficient for machine torque calculation. In some drives with large IM, air-gap flux is actually measured (Plounkett, 1979). In this particular case, it is a straightforward task to calculate machine torque based on the air-gap flux linkage projection orthogonal to the measured stator current vector. This is always a dynamic process, and the first order dynamics, with the time constant τ_f will be introduced to model this measurement. A standard singular perturbation argument involving estimation time constant ($\tau_f \rightarrow 0$) recovers the algebraic expression for the actual machine torque. In the stability analysis, both situations will therefore be discussed; in the first part the machine torque measurement will be assumed, and in in the second part the simple rotor flux linkage estimator will be introduced.

Indirect open-loop controller

In order to simultaneously satisfy requirements for high dynamic performance and maximal torque-per-amp ratio, the following indirect open-loop controller is proposed first, assuming nominal parameter case

$$\begin{aligned} \|i_s\| &= \tfrac{L_r}{M}\tfrac{|T_{el}|^\star}{|\hat{\psi}_\perp|} \qquad ; 0 \le \|i_s\| \le I_{\max} \\ \omega_r &= \tfrac{T_{el}^\star R_r}{\hat{\psi}_\perp^2 2} \qquad ; |\omega_r| \le |\omega_{\max}| \end{aligned} \tag{14}$$

where estimate $\hat{\psi}_\perp$ is obtained from the nominal rotor model (5). First control input $\|i_s\|$ is obtained from the equation for the machine torque (6) while the second input ω_r is derived from the instantaneous power equilibrium $\|i_s\|^2 R_r/2 = T_{el}\omega_r$ that is valid along the boundary of sector I. For nominal parameter case the control (14) assures the best possible performance, forcing the rotor flux trajectory to move along the the boundary of sector I for all required torques (except for zero initial condition in rotor flux linkage vector). The growth of the machine torque starting from zero initial condition in the rotor flux linkage vector depends on the maximal available stator current magnitude $I_{\max}$ and maximal rotation speed $\omega_{\max}$. After transients, ω_r converges to τ_r^{-1} satisfying equilibrium conditions (11) and (12). Assuming nominal parameters simple rotor flux linkage estimator is introduced

$$\begin{aligned} \dot{\hat{\psi}}_I &= -\tfrac{1}{\tau_r}\hat{\psi}_I + \omega_r \hat{\psi}_\perp + \tfrac{M}{\tau_r}\|i_s\| \qquad ; \hat{\psi}_I(0) = 0 \\ \dot{\hat{\psi}}_\perp &= -\tfrac{1}{\tau_r}\hat{\psi}_\perp - \omega_r \hat{\psi}_I \qquad ; \hat{\psi}_\perp(0) = 0 \end{aligned} \tag{15}$$

Defining the estimation errors

$$\begin{aligned} e_I &= \psi_I - \hat{\psi}_I \\ e_\perp &= \psi_\perp - \hat{\psi}_\perp \end{aligned}$$

Straightforward computations show that estimation errors satisfy the equations

$$\begin{aligned} \dot{e}_I &= -\tfrac{1}{\tau_r}\, e_I + \omega_r\, e_\perp \\ \dot{e}_\perp &= -\tfrac{1}{\tau_r}\, e_\perp - \omega_r\, e_I \end{aligned} \tag{16}$$

It is easy to show that (16) is globally exponentially stable with Lyapunov function $V_o = \frac{1}{2}e_I^2 + \frac{1}{2}e_\perp^2$, and an estimate of the machine torque is obtained as

$$\hat{T}_{el} = -\frac{M}{L_r}\hat{\psi}_\perp \|i_s\| \tag{17}$$

If the rotor time constant τ_r^{-1} is considered as uncertain parameter due to variations in the rotor resistance, estimate $\widehat{\tau}_r$ is used in the perturbed estimator

$$\begin{aligned} \dot{\hat{\psi}}_I &= -\tfrac{1}{\widehat{\tau}_r}\, \hat{\psi}_I + \omega_r\, \hat{\psi}_\perp + \tfrac{M}{\widehat{\tau}_r}\|i_s\| \qquad ; \hat{\psi}_I(0) = 0 \\ \dot{\hat{\psi}}_\perp &= -\tfrac{1}{\widehat{\tau}_r}\, \hat{\psi}_\perp - \omega_r\, \hat{\psi}_I \qquad ; \hat{\psi}_\perp(0) = 0 \end{aligned} \tag{18}$$

Consequently the open-loop control (14) will shift the equilibrium point away from the boundary of sector I, additionally steady state error in the estimated machine torque will be observed

$$\begin{aligned} |\overline{\hat{\psi}}_\perp| = \overline{\hat{\psi}}_I &= \sqrt{\tfrac{|T_{el}^\star| L_r}{2}} \\ \overline{\psi}_I &= \tfrac{L_r}{1+\tau_r^2/\widehat{\tau}_r^2}\, \tfrac{|T_{el}^\star|}{|\hat{\psi}_\perp|} \\ |\overline{\psi}_\perp| &= \tfrac{\tau_r}{\widehat{\tau}_r}\overline{\psi}_I \\ \overline{\hat{T}}_{el} &= 2\tfrac{\tau_r \widehat{\tau}_r}{\tau_r^2+\widehat{\tau}_r^2}\, T_{el}^\star \end{aligned} \tag{19}$$

Direct open-loop controller

To reduce the influence of parameter perturbation we propose a more efficient procedure to estimate torque producing flux component. Instead of using rotor model based perturbed estimator (15), consider the stator voltage equation in the stationary reference frame

$$\widehat{\psi}_s = \int_0^t (u_s - R_s i_s) d\tau \qquad ; \widehat{\psi}_s(0) = 0 \tag{20}$$

where $u_s = [u_\alpha, u_\beta]^{\mathrm{T}}, i_s = [i_\alpha, i_\beta]^{\mathrm{T}}, \psi_s = [\psi_\alpha, \psi_\beta]^{\mathrm{T}}$ and R_s is the stator resistance. Expressing stator current and flux linkage vectors in the polar coordinates $\|i_s\| = \sqrt{i_\alpha^2 + i_\beta^2}, \varphi_i = \tan^{-1}(i_\beta / i_\alpha)$ and $\|\widehat{\psi}_s\| = \sqrt{\widehat{\psi}_\alpha^2 + \widehat{\psi}_\beta^2}, \varphi_\psi = \tan^{-1}(\widehat{\psi}_\beta / \widehat{\psi}_\alpha)$, torque producing flux linkage component $\widehat{\psi}_{eff}$ that is orthogonal to the stator current vector is obtained by using a simple transformation

$$\widehat{\psi}_{eff} = \|\widehat{\psi}_s\| \sin(\varphi_i - \varphi_\psi) \tag{21}$$

from where also the torque estimate can be calculated as $\widehat{T}_{el} = -\|i_s\|\widehat{\psi}_{eff}$. Estimation of the ψ_{eff} requires knowledge of the stator voltage vector u_s. If the corresponding voltage sensor is available, stator voltage is measured. In the opposite case, the reference voltages obtained from the current controllers could be used instead. A direct version of the open-loop torque

controller (14) could therefore be rewritten as

$$\begin{aligned} \|i_s\| &= \frac{|T_{el}|^\star}{|\hat{\psi}_{eff}|} \qquad ; 0 \le \|i_s\| \le I_{\max} \\ \omega_r &= \frac{T_{el}^\star R_r}{\hat{\psi}_{eff}^2 2} \qquad ; |\omega_r| \le |\omega_{\max}| \end{aligned} \tag{22}$$

Note that the method of using torque producing flux linkage components $\widehat{\psi}_\perp$ or $\widehat{\psi}_{eff}$ for the torque control is a obvious consequence of selected reference frame aligned with the stator current vector.

Indirect closed-loop controller

To assure ultimate steady-sate accuracy in the estimated machine torque a feedback version of the open-loop controller (14) based on the torque error $\widetilde{T}_{el} = T_{el}^\star - \widehat{T}_{el}$ is proposed in the following form

$$\begin{aligned} \|i_s\| &= \frac{L_r}{M}\frac{|T_{el}|^\star}{|\hat{\psi}_\perp|} \qquad ; 0 \le \|i_s\| \le I_{\max} \\ \dot{v} &= k_i \widetilde{T}_{el} \qquad ; k_i > 0, v(0) = 0, |v| \le \hat{\tau}_r^{-1} \\ \omega_r &= v + k_p \widetilde{T}_{el} \qquad ; k_p > 0, |\omega_r| \le |\omega_{\max}| \end{aligned} \tag{23}$$

Calculating the fifth order feedback system based on rotor model (5), perturbed estimator (18) and control law (23) results in

$$\begin{aligned} \dot{\psi}_I &= -\tau_r^{-1}\psi_I + (v + k_p\widetilde{T}_{el})\psi_\perp + L_r\tau_r^{-1}\frac{|T_{el}^\star|}{|\hat{\psi}_\perp|} \\ \dot{\psi}_\perp &= -\tau_r^{-1}\psi_\perp - (v + k_p\widetilde{T}_{el})\psi_I \\ \dot{\hat{\psi}}_I &= -\hat{\tau}_r^{-1}\hat{\psi}_I + (v + k_p\widetilde{T}_{el})\hat{\psi}_\perp + L_r\hat{\tau}_r^{-1}\frac{|T_{el}^\star|}{|\hat{\psi}_\perp|} \\ \dot{\hat{\psi}}_\perp &= -\hat{\tau}_r^{-1}\hat{\psi}_\perp - (v + k_p\widetilde{T}_{el})\hat{\psi}_I \\ \dot{v} &= k_i\widetilde{T}_{el} \end{aligned} \tag{24}$$

with unique equilibrium point

$$\begin{aligned} \overline{\psi}_I &= \sqrt{\frac{\hat{\tau}_r^3|T_{el}^\star|L_r}{\tau_r\hat{\tau}_r^2+\tau_r^3}} \\ |\overline{\psi}_\perp| &= \frac{\tau_r}{\hat{\tau}_r}\overline{\psi}_I \\ |\overline{\hat{\psi}}_\perp| &= \overline{\hat{\psi}}_I = \sqrt{\frac{|T_{el}^\star|L_r}{2}} \\ \overline{\omega}_r &= \overline{v} = \hat{\tau}_r^{-1} \\ \overline{\hat{T}}_{el} &= T_{el}^\star \end{aligned} \tag{25}$$

Consequently, the actual rotor flux linkage vector will be forced to move slightly away from boundary into sector I provided $\hat{\tau}_r^{-1} \le \tau_r^{-1}$. Linearizing feedback system (24) around equilibrium point (25), we observe that rotor and estimator dynamics are governed by the stable eigenvalues $\lambda_{1,2} = -\tau_r^{-1} \pm j\hat{\tau}_r^{-1}$ and $\lambda_{3,4} = -\hat{\tau}_r^{-1} \pm j\hat{\tau}_r^{-1}$. Since the term $|T_{el}^\star|/|\hat{\psi}_\perp|$ is bounded by controller construction the feedback system (24) is locally stable. the restriction of local stability could eventually be relaxed by introducing Lyapunov function candidate $V_c = 1/2(\psi_I^2 + \psi_\perp^2 + \hat{\psi}_I^2 + \hat{\psi}_\perp^2 + v^2)$. Calculating the time derivative of V_c along the solution

of (24) gives

$$\dot{V}_c = -\tau_r^{-1}(\psi_I^2 + \psi_\perp^2 - \frac{\psi_I L_r |T_{el}^\star|}{|\hat{\psi}_\perp|}) - \hat{\tau}_r^{-1}(\hat{\psi}_I^2 - \hat{\psi}_\perp^2 + \frac{\hat{\psi}_I L_r |T_{el}^\star|}{|\hat{\psi}_\perp|}) \tag{26}$$

As ψ_I and $\hat{\psi}_I$ are positive semi-definite due to chosen reference frame, the derivative of V_c is obviously negative definite.

Full information controller

Assuming that the electro-mechanical torque (6) is measured, the following dynamic controller is proposed[1]

$$\begin{aligned} \omega_r &= \text{sat}_{[-k_4,k_4]}\left(k_p\,\widetilde{T}_{el} + v\right) \\ \| \, i_s \, \| &= -2\,\tfrac{\hat{\tau}_r}{M}\,\psi_\perp^\star\,\omega_r \\ \dot{\widetilde{T}}_{el} &= \tau_f^{-1}\left(T_{el}^\star - \widetilde{T}_{el} - T_{el}\right) \\ \dot{v} &= k_i\,\widetilde{T}_{el}, \end{aligned} \tag{27}$$

where k_p, k_i, $\tau_f \ll \tau_r$ and k_4 are positive design constants, $\hat{\tau}_r$ is an estimate of the rotor time constant and $\widetilde{T}_{el}$ is an auxiliary state.
The closed–loop dynamics yields

$$\begin{aligned} \dot{\psi}_I &= -\tfrac{1}{\tau_r}\,\psi_I + (k_p\,\widetilde{T}_{el} + v)\,\psi_\perp - 2\,\tfrac{\hat{\tau}_r}{\tau_r}\,\psi_\perp^\star\,(k_p\,\widetilde{T}_{el} + v) \\ \dot{\psi}_\perp &= -\tfrac{1}{\tau_r}\,\psi_\perp - (k_p\,\widetilde{T}_{el} + v)\,\psi_I \\ \dot{\widetilde{T}}_{el} &= \tau_f^{-1}\,\left[T_{el}^\star - \widetilde{T}_{el} - 2\,\tfrac{\hat{\tau}_r}{L_r}\,\psi_\perp^\star\,\psi_\perp\,(k_p\,\widetilde{T}_{el} + v)\right] \\ \dot{v} &= k_i\,\widetilde{T}_{el} \end{aligned} \tag{28}$$

thus, the closed–loop equilibria are the solutions of the following equations

$$\begin{aligned} 0 &= -\tfrac{1}{\tau_r}\,\psi_{Ie} + v_e\,\psi_{\perp e} - 2\,\tfrac{\hat{\tau}_r}{\tau_r}\,\psi_{\perp e}\,v_e \\ 0 &= -\tfrac{1}{\tau_r}\,\psi_{\perp e} - v_e\,\psi_{Ie} \\ 0 &= \tau_f^{-1}\,\left[T_{el}^\star - 2\,\tfrac{\hat{\tau}_r}{L_r}\,\psi_\perp^\star\,\psi_{\perp e}\,v_e\right] \end{aligned} \tag{29}$$

From the first two equations of (29) we obtain ψ_{Ie} and $\psi_{\perp e}$. Now, replacing ψ_{Ie}, $\psi_{\perp e}$ and $\psi_\perp^\star$ into the third relation and considering $|T_{el}^\star| = \text{sign}(T_{el}^\star)\,T_{el}^\star$, we obtain the following cubic polynomial with respect to v_e

$$f(v_e) = 1 + {v_e}^2\,\tau_r^2 - 2\,\text{sign}(T_{el}^\star)\,\tau_r\,\hat{\tau}_r^2\,v_e^3 = 0 \tag{30}$$

Hence, the number of equilibrium points of (28) is determined by the number of real roots of the polynomial (30). Basic computations show that for $T_{el}^\star > 0$ ($T_{el}^\star < 0$), $f(v_e)$ has a minimum

[1] With $\text{sat}_{[a,b]}(u) = \begin{cases} u \text{ if } a \le u \le b \\ a \text{ if } u < a \\ b \text{ if } u > b \end{cases}$.

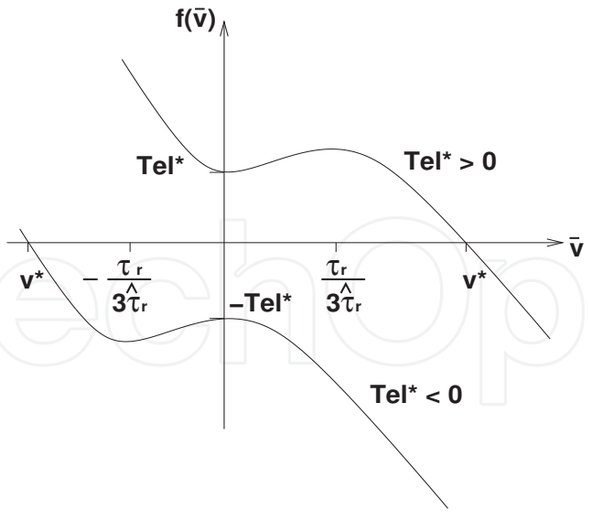

Fig. 3. Equilibrium points of $f(v_e)$.

(maximum) at $v_{e_1} = 0$ and a maximum (minimum) at $v_{e_2} = \frac{1}{3}\frac{\tau_r}{\hat{\tau}_r^2}$ ($v_{e_2} = -\frac{1}{3}\frac{\tau_r}{\hat{\tau}_r^2}$), see Fig. 3; moreover, $f(v_{e_2}) > f(v_{e_1}) > 0$ ($f(v_{e_2}) < f(v_{e_1}) < 0$). Thus, it can be concluded that (30) has only one real root so that the closed-loop dynamics (28) has a unique equilibrium point given by

$$\begin{bmatrix} \psi_{Ie} \\ \psi_{\perp e} \\ \widetilde{T}_{el} \\ v_e \end{bmatrix} = \begin{bmatrix} -\frac{2\,\hat{\tau}_r\, v^\star\, \psi_\perp^\star}{1+v^{\star 2}\,\tau_r^2} \\ \frac{2\,\tau_r\,\hat{\tau}_r\, v^{\star 2}\,\psi_\perp^\star}{1+v^{\star 2}\,\tau_r^2} \\ 0 \\ v^\star \end{bmatrix} \tag{31}$$

with $v^\star$ the unique real root of (30). It is important to point out that, for small values of $\hat{\tau}_r$, with respect to τ_r the value of $v^\star$ increases and the risk of stalling also increases since $\omega_r^\star = v^\star$. In order to avoid this risk, we need to choose $\hat{\tau}_r$ larger than τ_r, thus keeping $v^\star$ small, (see Fig. 3). A detailed stability analysis is given in App.I.

5. Current control

The task of the inner current controllers is demanding since reference tracking, disturbance suppression and voltage drop compensation of the VSI must be achieved simultaneously. Note that inverse mapping between the current vector magnitude $\|i_s\|$ and the voltage u_I is characterized by perturbed first-order dynamics and that inverse mapping between ω_i and voltage $u_\perp$ is purely algebraic and nonlinear. Before introducing the current controllers a physical interpretation of the nominal mapping $\|i_s\|, \omega_i \to u_I, u_\perp$ is given.
Analyzing the stator equations of (4) in polar form

$$\begin{aligned} \dot{\|i_s\|} &= -\tau_\sigma^{-1}\|i_s\| + \tfrac{M}{L_\sigma L_r \tau_r}\psi_I + \omega_m \tfrac{M}{L_\sigma L_r}\psi_\perp + \tfrac{1}{L_\sigma}u_I \\ \dot{\theta}_i = \omega_i &= -\omega_m \tfrac{M}{L_\sigma L_r}\tfrac{\psi_I}{\|i_s\|} + \tfrac{M}{L_\sigma L_r \tau_r}\tfrac{\psi_\perp}{\|i_s\|} + \tfrac{1}{L_\sigma\|i_s\|}u_\perp \end{aligned} \tag{32}$$

and assuming synchronous operation first, when stator current vector and rotor flux linkage vector are aligned and characterized by the conditions $\omega_r = 0 \rightarrow T_{el} = 0, \psi_\perp = 0$ and $\omega_m \neq 0, \|i_s\| \neq 0 \rightarrow \omega_i = \omega_m$, $\psi_I \neq 0$, the required steady state voltage vector can be expressed as

$$\begin{aligned} u_I &= (R_\sigma - \tfrac{M^2}{L_r \tau_r})\|i_s\| \\ u_\perp &= (L_\sigma + \tfrac{M^2}{L_r})\|i_s\|\omega_m \end{aligned} \tag{33}$$

where the relation $\psi_I = M\|i_s\|$ is valid at synchronous operation. The control voltage u_I therefore influences only the flux linkage magnitude while $u_\perp$ is needed to enable synchronous rotation of the current vector. On the other hand, if the machine rotor is locked ($\omega_m = 0 \rightarrow \omega_i = \omega_r$) and the maximmum torque-per-amp operation is achieved ($\omega_r = \tau_r^{-1}$), the corresponding control voltage components are obtained in the form

$$\begin{aligned} u_I &= (R_\sigma - \tfrac{M^2}{2L_r \tau_r})\|i_s\| \\ u_\perp &= (L_\sigma + \mathrm{sign}(T_{el})\tfrac{M^2}{2L_r})\|i_s\|\omega_r \end{aligned} \tag{34}$$

where the relations $\psi_I = \|i_s\|M/2$ and $|\psi_\perp| = \psi_I$ were considered. In general, when the machine is rotated at a certain mechanical speed and an arbitrary electrical torque is generated, simultaneously satisfying maximum torque-per-amp requirement, the control voltage cannot be expressed simply as a superposition of (33) and (34) since flux linkage vector changes its magnitude and relative position between any steady state operation point. Control voltage vector, assuming operation at maximal torque-per-amp ratio $\omega_r = \tau_r^{-1}$ and considering that $\omega_i = \omega_m + \omega_r$, can therefore be calculated as

$$\begin{aligned} u_I &= (R_\sigma + (\mathrm{sign}(T_{el})\omega_m - \omega_r)\tfrac{M^2}{2L_r})\|i_s\| \\ u_\perp &= (L_\sigma + \tfrac{M^2}{2L_r})\|i_s\|\omega_m + (L_\sigma + \mathrm{sign}(T_{el})\tfrac{M^2}{2L_r})\|i_s\|\omega_r \end{aligned} \tag{35}$$

Note that both voltage components in (35) are expressed with known or measured quantities and that u_I predominantly changes rotor flux linkage magnitude and that $u_\perp$ influences the angle between the stator current vector and rotor flux linkage vector. Both voltages also define the steady state lower bound for u_I and upper bound for $u_\perp$ if stable operation inside sector I is supposed to be achieved. It is clear that the control voltage component $u_\perp$ is significant with respect to transient torque response, torque-per-amp ratio and stability. Poorly damped oscillatory torque responses are obtained if the control voltage $u_\perp$ is too high. In an extreme case, instability could even due to stall, as the angle between the stator current vector and the rotor flux linkage vector approaches $\pm\pi/2$. In the opposite case, when the rotation speed is too small, the angle between the stator current and the rotor flux linkage vectors is also small. The machine is therefore forced to operate with an unnecessarily large rotor flux linkage. Poor torque-per-amp ratio is the obvious consequence although the required torque is generated. It should be pointed out that the inverse mapping $\|i_s\|, \omega_i \rightarrow u_I, u_\perp$ is quite sensitive in practical implementation due to the partially algebraic plant nature, influence of the signal noise, parameter uncertainty and VSI operation. To avoid algebraic loops and obtain symmetrical current control structure with simple tuning rules and sufficient robustness, the stator equations of (4) are transformed into the rotor reference frame.

Current controllers in rotor reference frame

The task of current controller in the rotor reference frame is the mapping of reference currents $i_\gamma^\star$ and $i_\delta^\star$ into machine voltages u_γ and u_δ. The reference currents $i_\gamma^\star$ and $i_\delta^\star$ are obtained from torque controller output as:

$$\begin{aligned} \theta_r &= \int_0^t \omega_r(\tau)d\tau + \vartheta_f \quad ;\theta_r(0) = 0 \\ i_\gamma^\star &= \|i_s\|\cos(\theta_r) \\ i_\delta^\star &= \|i_s\|\sin(\theta_r) \end{aligned} \tag{36}$$

where feed-forward angle θ_f can be set as:

$$\theta_f = -\text{sign}(T_{el}^\star)\frac{\pi}{4} \tag{37}$$

The angle θ_f offers an addition degree of freedom in the torque control providing phase modulation of the stator current vector, while amplitude and frequency modulation are provided by the torque controller. This additional input can be used for fast (almost instantaneous) angle changes between the stator current vector and the rotor flux linkage vector in the case of sign changes of the reference torque (active breaking). Stator equation in rotor reference frame is obtained in the vector form as:

$$\begin{aligned} \dot{i}_{\gamma,\delta} &= -\tau_\sigma^{-1}(\mathrm{J}\omega_m\tau_\sigma + 1)i_{\gamma,\delta} + \tfrac{M}{L_\sigma L_r \tau_r}(\mathrm{J}^T\omega_m\tau_r + 1)\psi_{\gamma,\delta} \\ &+ \tfrac{1}{L_\sigma}u_{\gamma,\delta} = (A + \mathrm{J}\omega_m)i_{\gamma,\delta} + Bu_{\gamma,\delta} + d \end{aligned} \tag{38}$$

where the influence of the rotor flux linkage is captured in the disturbance d. Based on the well justified time separation of the stator and rotor dynamics bounded disturbance d could be neglected since that stator current dynamic is predominantly driven by the eigenvalues of the time variant system matrix $\lambda_{1,2}(A) = -\tau_\sigma^{-1} \pm j\omega_m$. For the cross-coupling effects between the current components $i_{\gamma,\delta}$ due to the motion induced voltages $L_\sigma \mathrm{J}\omega_m i_{\gamma,\delta}$, time separation is not justified since this voltage can change as fast as the stator current. To obtain a satisfactory tracking performance, these terms must be considered in control design. Simple feed-forward compensation with opposite sign provides only moderate performance due to uncertainty in the estimation of machine leakage inductance L_σ. Introducing the current error $\widetilde{i}_{\gamma,\delta} = i_{\gamma,\delta}^\star - i_{\gamma,\delta}$ the PI controller using internal model principle is therefore proposed in the following form:

$$u_{\gamma,\delta} = k_{pi}\widetilde{i}_{\gamma,\delta} + k_{pi}k_{ii}\int_0^t (\frac{\mathrm{J}\omega_m}{k_{ii}} + 1)\widetilde{i}_{\gamma,\delta}d\tau \tag{39}$$

where $k_{pi}, k_{ii} > 0$ are free design parameters. Dynamic of the augmented system is therefore given as:

$$\begin{aligned} \dot{i}_{\gamma,\delta} &= A(\omega_m)i_{\gamma,\delta} + Bk_{pi}\widetilde{i}_{\gamma,\delta} + Bz \\ \dot{z} &= (k_{pi}k_{ii} + k_{pi}\mathrm{J}\omega_m)\widetilde{i}_{\gamma,\delta} \qquad ;z(0) = 0 \end{aligned} \tag{40}$$

By choosing $k_{ii} = \tau_\sigma^{-1}$ and setting $i^\star_{\gamma,\delta} = 0$ the closed loop system matrix is obtained in the form:

$$A_{cl}(\omega_m) = \begin{bmatrix} -\tau_\sigma^{-1} - \frac{k_{pi}}{L_\sigma} & \omega_m & \frac{1}{L_\sigma} & 0 \\ -\omega_m & -\tau_\sigma^{-1} - \frac{k_{pi}}{L_\sigma} & 0 & \frac{1}{L_\sigma} \\ -\frac{k_{pi}}{\tau_\sigma} & k_{pi}\omega_m & 0 & 0 \\ -k_{pi}\omega_m & -\frac{k_{pi}}{\tau_\sigma} & 0 & 0 \end{bmatrix} \tag{41}$$

For any constant ω_m corresponding closed-loop eigenvalues are:

$$\begin{aligned} \lambda_{1,2} &= -k_{pi}/L_\sigma \\ \lambda_{3,4} &= -\tau_\sigma^{-1} \pm j\omega_m \end{aligned} \tag{42}$$

The eigenvalues $\lambda_{1,2}$ define the dynamics of the stator current, while $\lambda_{3,4}$ are related with the dynamics of the auxiliary variable z.

6. Experimental results

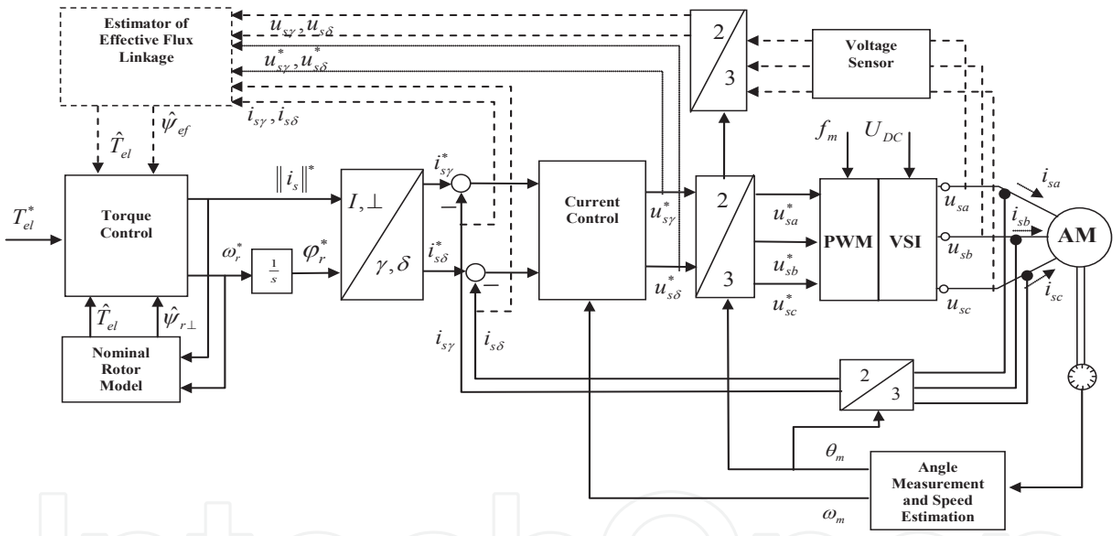

Fig. 4. Overall IM control scheme including torque controller, current controller, and estimator based on nominal rotor model. The dotted lines indicate advanced observers based on measured machine currents and voltages.

The experimental setup, motor data, along with the parameters of the torque and current controllers, are given in the Appendix. To avoid the danger of escaping, the DC motor was connected to the shaft. Breaking torque proportional to mechanical speed was generated ($t_l = k\omega_m$) so that the effect of the linear friction was simulated. In all experiments the most simple rotor flux estimator and torque calculator based on (15) and (17) were used

$$\begin{aligned} \dot{\widehat{\psi}}_I &= -\widehat{\tau}_r^{-1}\widehat{\psi}_I + \omega_r\widehat{\psi}_\perp + M\widehat{\tau}_r^{-1}\|i_s\| \\ \dot{\widehat{\psi}}_\perp &= -\widehat{\tau}_r^{-1}\widehat{\psi}_\perp - \omega_r\widehat{\psi}_I \\ \widehat{T}_{el} &= -\frac{M}{L_r}\widehat{\psi}_\perp\|i_s\| \end{aligned} \tag{43}$$

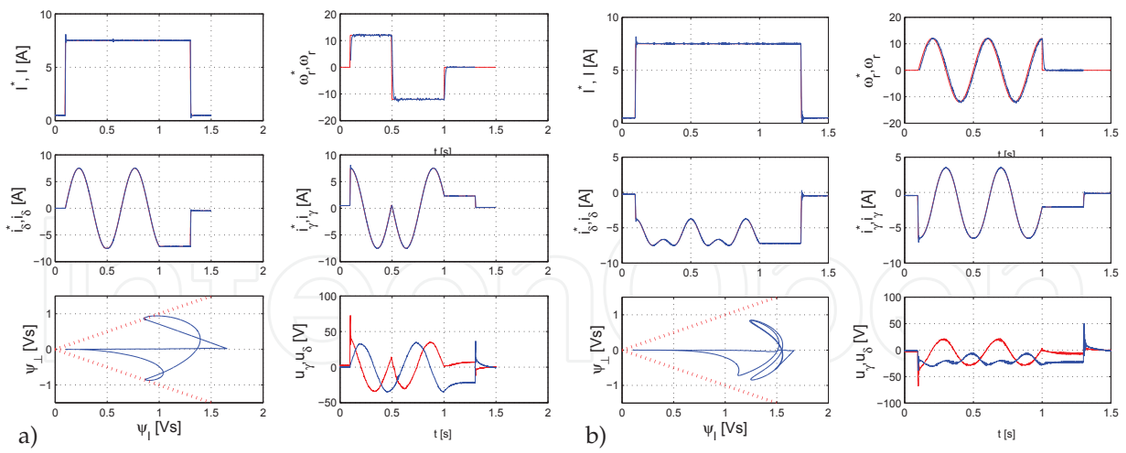

Fig. 5. Current control step response (a) and current control response to sinusoidal $\omega_r^\star$ (b).

where the actual stator current module $\|i_s\|$ and the relative speed ω_r were measured, and the nominal value of $\widehat{\tau}_r$ was used. The problem of all rotor based estimators is the uncertain rotor time constant $\widehat{\tau}_r$, completely neglecting the saturation effects influencing M and L_r. If the estimate of actual τ_r is wrong, than the steady-state error between estimated and actual machine torque occurs. Just to calibrate and verify steady-state torque and flux estimates at $\omega_m = 0 \rightarrow \omega_i = \omega_r$ (locked rotor), the torque sensor HBM-T20WN (10 Nm) was mounted between the IM and DC motor. By using torque sensor output T_{elm}, these estimates were corrected off-line by adjusting $\widehat{\tau}_r$

$$\begin{aligned} \widehat{\psi}_\perp &= -\tfrac{T_{elm}L_r}{M\|i_s\|} \\ \dot{\widehat{\psi}}_I &= -\widehat{\tau}_r{}^{-1}\widehat{\psi}_I - \tfrac{T_{elm}L_r}{M\|i_s\|}\omega_r + M\widehat{\tau}_r{}^{-1}\|i_s\| \qquad ;\widehat{\psi}_I(0) = 0 \end{aligned} \tag{44}$$

in such a way that $\widehat{T}_{el} \approx T_{elm}$ was achieved in steady-state. It should be pointed out that the estimated flux linkage component $\widehat{\psi}_I$ was used only to evaluate the transient performance and torque-per-amp ratio while the estimate $\widehat{\psi}_\perp$ was needed in torque calculation. The overall control scheme is shown in Fig. 4. The first two experiments show the performance of the current controller. Step changes in both reference current magnitude $\|i_s\|^\star$ and relative speed $\omega_r^\star$ are presented in Fig. 5a. Note that in all presented diagrams the current vector magnitudes $\|i_s\|^\star, \|i_s\|$ are denoted as $I^\star, I$) and machine torques $T_{el}^\star, \widehat{T}_{el}$ as $t_{el}^\star, t_{el}$. From the estimated rotor flux linkage trajectory it can be seen that the maximal torque-per-amp line is reached for each steady state as long as the condition $\omega_r \approx \tau_r^{-1}$ is satisfied. During transients, the flux linkage trajectory changes inside the desired operating sector I.

In Fig. 5b an experiment is shown where current vector magnitude was kept constant, while rotation speed ω_r was changed as a sinusoidal function with the magnitude between $\pm\tau_r^{-1}$. Since current magnitude is constant, the rotor flux linkage component ψ_I increases as ω_r decreases. Perfect current tracking could be observed in both experiments since reference and actual currents actually overlap.

The next few experiments show the responses of the torque controlled machine using nominal estimate of τ_r. Only positive torque reference was used during the first experiment in Fig. 6a, more demanding tracking task is presented in Fig. 6b, and torque reversal is shown in Fig. 7a.

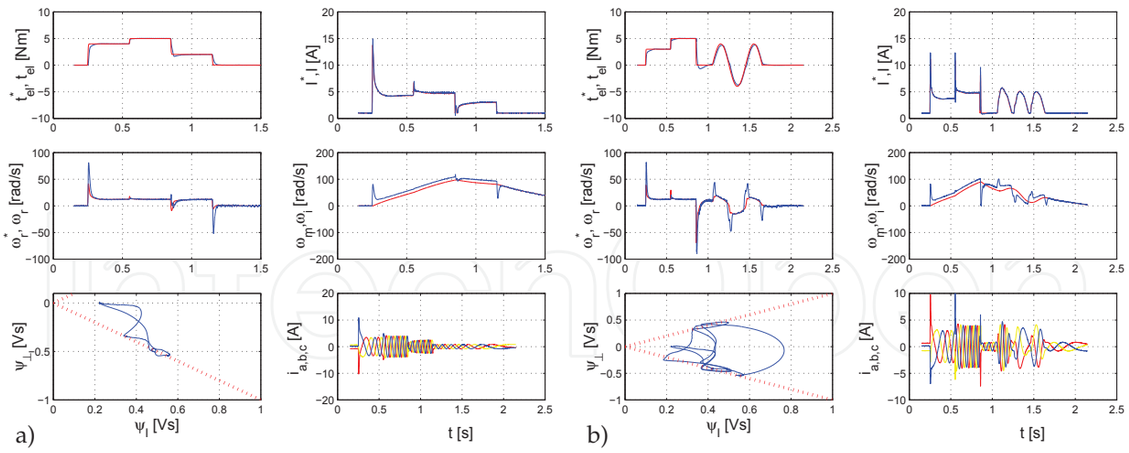

Fig. 6. Tracking of the positive torque reference (a) and tracking of the general torque reference (b).

The torque was built up completely after $\approx$ 50ms, starting practically from zero field; almost perfect tracking performance of the generated torque can be observed once a sufficient rotor field is established. The growth of ψ_I is slightly faster than growth of $\psi_\perp$, and the flux linkage trajectory is therefore forced to change inside the desired sector I. As the magnitude of the flux linkage vector components equalizes, the maximal torque-per-amp ratio operation is reached in all steady-states. In Fig. 7a the flux linkage trajectory also moves in sector II for a short period of time. This effect could be prevented by using "reset integrator" in torque controller. In Fig. 7b, an experiment is shown where short torque pulses were generated representing the high dynamic capability of the control scheme.
The next two experiments concern the perturbed rotor time constant case. The experiment in Fig. 8a was performed with $\hat{\tau}_r = 3\,\tau_r$, while the experiment in Fig. 8b was performed with $\hat{\tau}_r = 0.7\,\tau_r$. Note that in the first case the flux linkage trajectory is forced to move deeper in sector I, while in the second case the flux linkage trajectory moves also outside sector I. Decreasing the $\hat{\tau}_r$ further would therefore threat the stability while increasing $\hat{\tau}_r$ would just

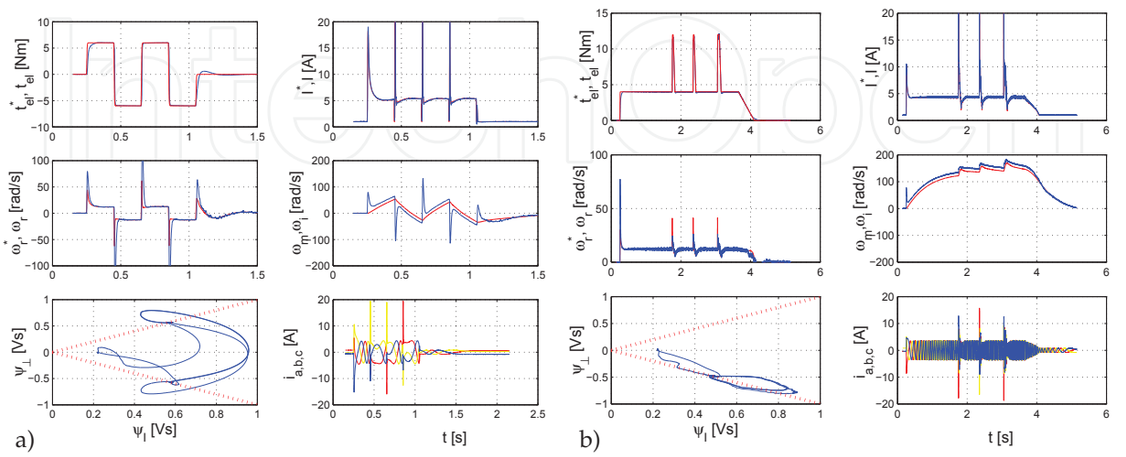

Fig. 7. Torque reversal (a) and generation of the torque pulses (b).

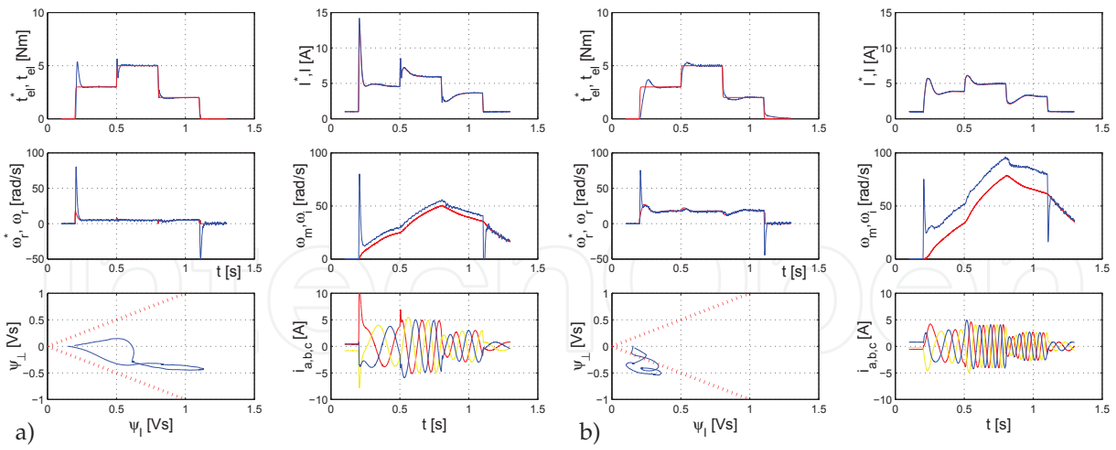

Fig. 8. Torque control with perturbed rotor time constant: $\hat{\tau}_r = 3\,\tau_r$ (a) and $\hat{\tau}_r = 0.7\,\tau_r$ (b).

increase the current vector magnitude and, consequently, the rotor field. In both cases stability was preserved, and the required torque was generated, however the maximal torque-per-amp operation was not reached.

The experiment in Fig. 9 shows that the proposed controller is able to handle operation at a higher rotor speed (approximately three times of the nominal speed). Experiments actually show responses similar to those in field weakening mode. Although the required torque is reduced, mechanical speed increases and reaches about three times the nominal speed. In all experiments could be observed how the stator current rotation speed changes relative to the rotor speed. During all steady-states, this relative speed equals the slip speed.

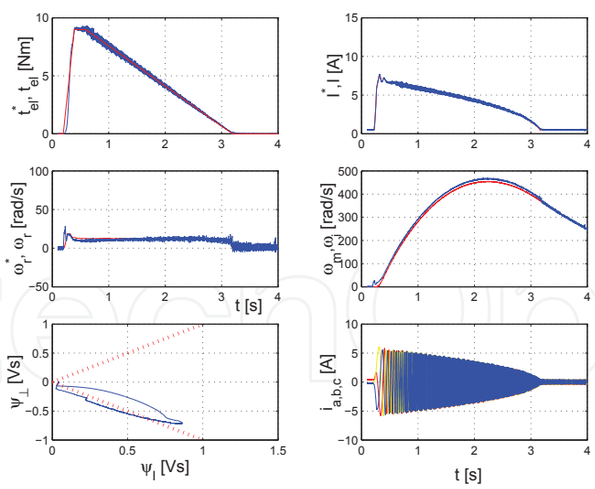

Fig. 9. Operation above nominal rotor speed.

7. Conclusion

The chapter presents a control scheme for torque control of IM based on a stator current vector reference frame. The overall design is motivated by physical interpretations of typical transient and steady-state IM phenomena rather than by concepts from abstract control

system theory. Nevertheless, the derived IM control based on introduced partial dynamic inversion enables an acceptable tracking performance, asymptotic stability for all physically feasible initial conditions, robustness with respect to rotor time constant perturbations and implicitly optimized torque-per-amp ratio. These properties were achieved while avoiding the FOC concept of a decoupled control based on rotor flux vector orientation. The key requirement in our solution is that all rotor flux linkage vector trajectories are implicitly restricted to the desired operating sector I and that, in steady-state, the trajectories end as close as possible to the maximal torque-per-amp line, simultaneously fulfilling basic control objectives. The proposed control assures implicit changes in the rotor flux vector without separate control actions. In addition, the proposed control is less sensitive with respect to saturation effects compared to other control schemes, whose reference frames are attached to the estimated machine fields. The implementation of the proposed control is possible on standard industrial hardware, assuming that the machine torque is calculated based on the flux estimate and measured current.

8. Appendix

Appendix I:

In order to analyze stability of the closed–loop dynamics, (28) can be written as

$$\dot{x} = A\,x + g(x) \tag{45}$$

where

$$x = \begin{bmatrix} \psi_I - \psi_{Ie} \\ \psi_\perp - \psi_{\perp e} \\ \widetilde{T}_{el} \\ \omega_r - v^* \end{bmatrix}, \quad g(x) = \begin{bmatrix} \widetilde{\psi}_\perp \\ -\widetilde{\psi}_I \\ -\frac{2\tau_r\,\psi_{\perp e}}{M\,\tau_f}\,\widetilde{\psi}_\perp \\ -\frac{2k_p\tau_r\,\psi_{\perp e}}{M\,\tau_f}\,\widetilde{\psi}_\perp \end{bmatrix} \widetilde{\omega}_r$$

$$A = \begin{bmatrix} -\frac{1}{\tau_r} & v^* & 0 & -\psi_{\perp e} \\ -v^* & -\frac{1}{\tau_r} & 0 & \frac{\psi_{\perp e}}{\tau_r\,v^*} \\ 0 & -\frac{2\tau_r\,v^*\,\psi_{\perp e}}{M\,\tau_f} & -\frac{1}{\tau_f} & -\frac{2\tau_r\,\psi_{\perp e}^2}{M\,\tau_f} \\ 0 & -\frac{2k_p\tau_r\,v^*\,\psi_{\perp e}}{M\,\tau_f} & k_i - \frac{k_p}{\tau_f} & -\frac{2k_p\tau_r\,\psi_{\perp e}^2}{M\,\tau_f} \end{bmatrix}$$

Straightforward computations show that the linear part of (45) is exponentially stable provided that $\tau_f < 1$ and $k_p \geq k_i\,\tau_f$. Stability of the linear part of (45) implies that there exist a positive definite matrix P such that

$$P\,A + A^\top P = -I$$

with I the identity matrix. Note that the time derivative of $V = x^\top P\,x$ along (45) gives

$$\dot{V} = -x^\top x + 2\,\widetilde{\omega}_r\,x^\top P\,G\,x$$

where

$$G = \begin{bmatrix} 0 & 1 & 0\ 0 \\ -1 & 0 & 0\ 0 \\ 0 & -\frac{2\tau_r\,\psi_{\perp e}}{M\,\tau_f} & 0\ 0 \\ 0 & -\frac{2k_p\tau_r\,\psi_{\perp e}}{M\,\tau_f} & 0\ 0 \end{bmatrix}$$

therefore, we have

$$\dot{V} \leq -\|x\|^2 + 2\,\bar{k}_4\,\|PG\|\,\|x\|^2$$

for all $|\widetilde{\omega}_r| < \bar{k}_4$ with $\bar{k}_4 = k_4 + |v^\star|$ and $\dot{V}$ is negative definite provided

$$\bar{k}_4 < \frac{1}{2\,\|PG\|} \tag{46}$$

Thus, it can be concluded that the dynamics (5) in closed–loop with the controller (27) is exponentially stable in the domain

$$D = \left\{ x \in R^4 \mid \sqrt{x_1^2 + x_2^2 + x_3^2 + \bar{k}_4^2} \leq r \right\}$$

An estimate of the region of attraction in the plane $\psi_I - \psi_\perp$ can be obtained as follows. Consider the positive definite function $V_1 = \frac{1}{2}\widetilde{\psi}_I^2 + \frac{1}{2}\widetilde{\psi}_\perp^2$ whose time derivative along (45) is given by

$$\dot{V}_1 = -\frac{1}{\tau_r}(\widetilde{\psi}_I^2 + \widetilde{\psi}_\perp^2) - \psi_\perp^\star\,\widetilde{\omega}_r\,\widetilde{\psi}_I + \frac{\psi_\perp^\star}{\tau_r\,v^\star}\widetilde{\omega}_r\,\widetilde{\psi}_\perp$$

from (46) we have

$$\dot{V}_1 \leq -\frac{1}{\tau_r}\|\widetilde{\psi}\|^2 + \frac{\bar{k}_4\,|\psi_\perp^\star|}{\tau_r\,v^*}\sqrt{1+\tau_r^2\,v^{\star 2}}\|\widetilde{\psi}\|$$

where $\widetilde{\psi} = [\,\widetilde{\psi}_I\ \widetilde{\psi}_\perp\,]$. Thus, $\dot{V}_1$ is negative definite provided

$$\|\widetilde{\psi}\| > \frac{\bar{k}_4\,|\psi_\perp^\star|}{v^*}\sqrt{1+\tau_r^2\,v^{\star 2}}$$

and an estimate of the domain of attraction $\Omega_c$is given as

$$\Omega_c = \{V_1(\widetilde{\psi}) = c\}$$

with $c > \frac{\bar{k}_4^2\,|\psi_\perp^{\star 2}|}{v^{*2}}(1+\tau_r^2\,v^{\star 2})$.

Remark. *It should be stressed, that in steady state, the controller output provides useful information for estimation of the rotor time constant. Note that, in steady state, we have access to $v^\star$ so that the only unknown in (30) is the rotor time constant, which can be computed as*

$$\tau_r = \begin{cases} \frac{\hat{\tau}_r^2\,v^{\star 2} + \sqrt{\hat{\tau}_r^4\,v^{\star 4} - 1}}{v^\star}, & \textit{for}\ \ T_{el}^\star > 0 \\ \frac{\hat{\tau}_r^2\,v^{\star 2} - \sqrt{\hat{\tau}_r^4\,v^{\star 4} - 1}}{v^\star}, & \textit{for}\ \ T_{el}^\star < 0 \end{cases} \tag{47}$$

Remark. *Figure 3 shoes that efficiency depends on the accuracy of the rotor time constant as any mismatch in the estimated rotor time constant $\hat{\tau}_r$ affects the magnitude of $v^\star$. Thus, recalling that $\omega_r^\star = v^\star$, the rotor dynamics (5) may not operate at the maximal torque per ampere ratio defined by (9); however stable operation is preserved.*

Stability analysis using estimated machine torque.
Simple computations show that by replacing the machine torque (6) with its estimated value (17) in (27) gives a closed–loop dynamics described by equations (45) perturbed by an additive term which is bounded by $\kappa\,|e_\perp|$ for a positive constant κ and it is exponentially decaying to zero. Consider now the Lyapunov function V and note that

$$\dot{V} \leq -\|x\|^2 + 2\,\bar{k}_4\,\|PG\|\,\|x\|^2 + \kappa\,\|P\|\,\|x\|\,|e_\perp| \leq \kappa\,\|P\|\,\|x\|\,|e_\perp| \tag{48}$$

for $\bar{k}_4$ satisfying (46). THE equation (48) implies that, along the trajectories of the closed–loop system with estimated electro-mechanical torque, V is bounded. As a result, $\|x\|$ is bounded and, converges to zero, since $e_\perp$ exponentially decays to zero.

Appendix II:

Beside the tested IM the experimental setup consisted of: a DSPACE DS1103 PPC Controller board, a host PC with installed development environment, an incremental encoder Iskra TELA TGR 10 with 2500 pulses per revolution, current sensors LEM LT 100-P, Semikron inverter (modules SKH1 22, SKM 50GB 123D and SKD 51/14, up to 800 V at the dc bus and currents up to 30 A RMS) and DC motor. The DSPACE DS 1103 PPC Controller board consists of: the IBM PowerPC 604e, the slave digital signal processor (DSP) TMS320F240, interfaces for incremental encoders, and AD and DA converters. Although ω_i can be obtained directly by (noisy) derivation of the current angle vector θ_i a second order observer as proposed in (Harnefors & Nee, 2000) was used. During the tests, data acquisition, transformations, and control were executed on the PowerPC, while the slave DSP was used for vector modulation running at 4 kHz. All experiments were performed with the sampling time of 250 μs. The program codes for the PowerPC and for the slave DSP were developed with Real Time Interface and Simulink.

Stator resistance	$R_s = 1.976\Omega$
Rotor resistance	$R_r = 2.91\Omega$
Mutual inductance	$M = 0.223$H
Stator inductance	$L_s = 0,2335$ H
Rotor inductance	$L_r = 0.2335$ H
Stator leakage inductance	$L_{s\sigma} = 0.0105$ H
Rotor leakage inductance	$L_{r\sigma} = 0.0105$ H
Number of pole pairs	$p = 2$
Nominal torque	$T_{el} = 10$ Nm

Table 1. Nominal motor data

k_p	15
k_i	800
τ_f	0.005s
Current bounds	$0.5 \leq \|i_s\| \leq 20$A
k_{pi}	20
k_{ii}	225.5

Table 2. Controller parameters

9. List of symbols

$i_{\alpha,\beta}, u_{\alpha,\beta}, \psi_{\alpha,\beta}$	components of stator current, stator voltage and rotor flux linkage vectors in stationary reference frame
$u_{I,\perp}, \psi_{I,\perp}$	parallel $(.)_I$ and orthogonal $(.)_\perp$ components of stator voltage and rotor flux linkage vectors
$i_{\gamma,\delta}, u_{\gamma,\delta}, \psi_{\gamma,\delta}$	components of stator current, stator voltage and rotor flux linkage vectors in rotor reference frame
$\|.\|$	norm L_2 of vectors or matrices
ω_m	rotor speed (mechanical)
ω_i	stator current vector rotation speed
$\omega_r = \omega_i - \omega_m$	relative rotation speed of stator current vector
θ_i	absolute stator current vector angle
θ_r	relative stator current vector angle
θ_f	feed-forward angle
M	mutual inductance
R_r, L_r	rotor resistance and self-inductance
$\tau_r = L_r/R_r$	rotor time constant
T_{el}, T_L	machine torque, load torque
J	drive inertia
R_s, L_s	stator resistance and self-inductance
$\tau_\sigma = L_\sigma/R_\sigma$	leakage time constant
$L_\sigma = L_s - (M)^2/L_r$	leakage inductance
$R_\sigma = R_s + (M/L_r)^2 R_r$	leakage resistance
$\mathrm{J} = [0, -1; 1, 0]$	2×2 rotation matrix
k_p, k_i, k_4	torque controller parameters
τ_f	torque estimator time constant
v	output from integral control action
k_{pi}, k_{ii}	current controller parameters
$(.)^\star, \widehat{(.)}, \widetilde{(.)}, \overline{(.)}$	reference values, estimated values, errors, steady state values
$(.)_e$	equilibrium values
$e_I, e_\perp$	rotor flux linkage estimation errors

10. References

Attaianese C., Nardi V., Perfetto A. & Tomasso G. (1999). Vectorial Torque Control: A Novel Approach to Torque and Flux Control of Induction Motor Drives, *IEEE Transactions on Industry Applications*, Vol. 35, No. 6, pp. 1399–1405.

Blaschke F. (1971). Das Prinzip der Feldorientierung, die Grundlage für die Transvektor-Regelung von Drehfeldmaschinen, *Siemens Zeitschrift*, Vol. 10, No. 45.

Bodson M. & Chiasson J. (1998). Differential-Geometric Methods for Control of Electric Motors, *International Journal of Robust and Nonlinear Control*, No. 8, pp. 927–952.

Briz F., Degner M.W., Diez A. & Lorenz R.D. (2002). Static and Dynamic Behavior of Saturation-Induced Saliencies and Their Effect on Carrier-Signal-Based Sensorless AC Drives, *IEEE Transactions on Industry Applications*, Vol. 38, No. 3, pp. 670–678.

Brockett R. (1996). Characteristic Phenomena and Model Problems in Nonlinear Control, *IFAC, 13th Triennial World Congres, San Francisco*, 2b II, pp. 257–262.

Grčar B., Cafuta P., Štumberger G., Stankovič A., Hofer A. (2011). Non-holonomy in Induction Torque Control, *IEEE Transactions on control System Technology*, Vol. 19, No. 2, pp. 367–375.

Chakraborty C., Hori Y. (2003). Fast Efficiency Optimization Techniques for the Indirect Vector-Controlled Induction Motor Drives, *IEEE Transactions on Industry Applications*, Vol. 39, No. 4, pp. 1070–1076.

Chiasson J. (1998). A New Approach to Dynamic Feedback Linearization Control of an Induction Motor, *IEEE Transactions on Automatic Control*, Vol. 43, No. 3, pp. 391–396.

Depenbrock M. (1986). Direct Self-Control (DSC) of Inverter-Fed Induction Machine, *IEEE Transactions on Industry Applications*, Vol. IA-22, No. 5, pp. 820–827.

Harnefors L., Nee H.P. (2000). A General Algorithm for Speed and Position Estimation of AC Motors, *IEEE Transactions on Indusrtial Electronics*, Vol. 47, No. 1, pp. 77–83.

Krause P.C. (1986). *Analysis of Electric Machinery*, McGraw-Hill.

Marino R., Peresada S. & Tomei P. (1999). Global Adaptive Output Feedback Control of Induction Motors with Uncertain Rotor Resistance, *IEEE Transactions on Automatic Control*, Vol. 44, No. 5, pp. 967–980.

Martin P., Rouchon P. (1996). Flatness and Sampling Control of Induction Motor, *IFAC, 13th Triennial World Congres, San Francisco*, 2b 27 2, pp. 389–394.

Ortega R., Loria A., Nicklasson P.J. & Siera-Ramirez H. (1998). *Passivity-based Control of Euler-Lagrange Systems*, Springer-Verlag, Berlin.

Ortega R., Barabanov N., Escobar G. (2000). Direct Torque Control of Induction Motors: Stability Analysis and Performance Improvement, *IEEE Transactions on Automatic Control*, Vol. 46, No. 8, pp. 967–980.

Peresada S., Tilli A., Tonielli A. (2003). Theoretical and Experimental Comparison of Indirect Field-Oriented Controllers for Induction Motors, *IEEE Transactions on Power Electronics*, Vol. 18, No. 1, pp. 151–163.

Plounkett A.B., D'Atre J.D., Lipo T.A. (1979). Synchronous Control of a Static AC Induction Motor Drive, *IEEE Transactions on Indusrty Applications*, Vol. 5, No. 4, pp. 430–437.

Takagashi I., Noguchi T. (1986). A New Quick-Response and High-Efficiency Control Strategy of an Induction Motor, *IEEE Transactions on Industry Applications*, Vol. IA-22, No. 5, pp. 820–827.

Vas P. (1998). *Sensorless Vector and Direct Torque Control*, Oxford University Press, Oxford.

Verghese G.C., Sanders S.R. (1988) Observers for Flux Estimation in Induction Machines, *IEEE Transactions on Industrial Electronics*, Vol. 35, No. 1, pp. 85–93.

Cutting Edge Research in New Technologies

Edited by Prof. Constantin Volosencu

ISBN 978-953-51-0463-6
Hard cover, 346 pages
Publisher InTech
Published online 05, April, 2012
Published in print edition April, 2012

The book "Cutting Edge Research in New Technologies" presents the contributions of some researchers in modern fields of technology, serving as a valuable tool for scientists, researchers, graduate students and professionals. The focus is on several aspects of designing and manufacturing, examining complex technical products and some aspects of the development and use of industrial and service automation. The book covered some topics as it follows: manufacturing, machining, textile industry, CAD/CAM/CAE systems, electronic circuits, control and automation, electric drives, artificial intelligence, fuzzy logic, vision systems, neural networks, intelligent systems, wireless sensor networks, environmental technology, logistic services, transportation, intelligent security, multimedia, modeling, simulation, video techniques, water plant technology, globalization and technology. This collection of articles offers information which responds to the general goal of technology - how to develop manufacturing systems, methods, algorithms, how to use devices, equipments, machines or tools in order to increase the quality of the products, the human comfort or security.

INTECH
open science | open minds

InTech Europe
University Campus STeP Ri
Slavka Krautzeka 83/A
51000 Rijeka, Croatia
Phone: +385 (51) 770 447
Fax: +385 (51) 686 166
www.intechopen.com

InTech China
Unit 405, Office Block, Hotel Equatorial Shanghai
No.65, Yan An Road (West), Shanghai, 200040, China
中国上海市延安西路65号上海国际贵都大饭店办公楼405单元
Phone: +86-21-62489820
Fax: +86-21-62489821

IntechOpen